Loss-Minimization Control of Vector-Controlled Induction Motor Drives

Sheng-Ming Yang, *Member, IEEE* and Feng-Chieh Lin

***Abstract*--It is well know that the efficiency of induction motor drive under partial load can be improved via manipulation of its field. Among the numerous loss-minimization schemes proposed previously, the scheme that uses motor power factor as the main control variable has the advantages of high sensitivity and ease of implementation. But the problem of how the optimal power factor commands can be generated is not well documented. In this paper, a scheme that uses power factor control with automatic measurement of the minimum-loss power factor commands is proposed. A fuzzy logic compensator is included in the controller to improve the accuracy of the generated commands. The scheme is simple for implementation and does not require an a priori knowledge of motor parameters. Experimental results have validated the effectiveness of this scheme to minimize the motor operating losses.**

***Index Terms*-- induction motor, loss minimization, vector control, fuzzy Logic, auto-commissioning**

I. INTRODUCTION

Approximately half of electric energy is consumed by electric motors in the world today, and majority of them are induction motors. Because the efficiency of induction motor varies significantly with its operating condition, energy savings in the operating loss can be obtained with optimal control strategies. The operating loss in an induction motor is consisted of: 1) stator and rotor copper losses, 2) core losses and 3) mechanical losses. At light loads, motor efficiency decreases due to an unbalance between the copper and the core losses. Hence energy saving can be achieved by proper selection of the flux level in the motor.

Many minimum-loss control schemes have been reported previously. A popular method is to keep the output power constant and searching for the operating point where the input power has a minimum [1]. The operating point can be varied by adjusting the V/f ratio [2], application of fuzzy logic control to adjust the magnetizing current [3], or by adaptive control [4]. The minimum-loss operating condition is obtained by iteratively changing the flux level in small steps until the minimum input power is detected. The main advantage of search control is that an a priori knowledge on motor parameters is not required. However, because the relationship between input power and flux near the minimum-loss point is fairly flat, the input power must be accurately measured to prevent oscillatory response in the control.

Because the motor losses in the direct and the quadratic axes are balanced when the motor is at its minimum-loss point, a feedback controller can be used to force the motor to operate at this point [5-8]. This scheme is mostly used in the variable voltage/variable frequency drives to find the optimal V/f ratio [7]. Similarly, the motor slip can also be used as the primary controlled variable [9-10]. Though these minimum-loss control schemes are simple for implementation, its performance is depending on the accuracy of the motor model.

The motor power factor can also be used as the main control variable for efficiency optimization [11-12]. In this method, the motor operating loss is minimized by indirectly controlling motor flux in order to balance the copper and the core losses. The power factor control scheme has the advantage that the controller can be stabilized easily and the motor parameter information is not required. However, generation of the optimal power factor command remain tedious and restrictive because experimental methods were generally used [12].

In this paper, a minimum-loss control scheme that uses power factor as the main control variable for vector-controlled induction motor drives is proposed. The controller can generate minimum-loss power factor commands without an a priori knowledge of motor parameters. A fuzzy logic compensator is also included in the control scheme to improve the accuracy of the generated power factor commands.

II. MOTOR MODEL

The d-q equations for a three-phase squirrel cage induction motor in the synchronous rotating frame can be written as

$$v_{qs}^e = r_s i_{qs}^e + p\lambda_{qs}^e + \omega_e \lambda_{ds}^e \quad (1)$$

$$v_{ds}^e = r_s i_{ds}^e + p\lambda_{ds}^e - \omega_e \lambda_{qs}^e \quad (2)$$

$$0 = r_r i_{qr}^e + p\lambda_{qr}^e + (\omega_e - \omega_r)\lambda_{dr}^e \quad (3)$$

$$0 = r_r i_{dr}^e + p\lambda_{dr}^e - (\omega_e - \omega_r)\lambda_{qr}^e \quad (4)$$

where $v_{qs}^e, v_{ds}^e, i_{qs}^e, i_{ds}^e, i_{qr}^e, i_{dr}^e, \lambda_{qs}^e, \lambda_{ds}^e, \lambda_{qr}^e, \lambda_{dr}^e$ are the *q-d* axis stator voltages, stator and rotor currents, stator and rotor flux, respectively; r_s, r_r are the stator and rotor resistance; ω_e is the frequency, ω_r is the rotor electrical speed, and p is the derivative operator. The operating loss of an induction motor is consisted of the stator and rotor copper losses, the core losses and, and the mechanical losses. Mechanical losses are neglected since they are small compared to the other losses. Core losses are consisted of Eddy current and hystersis losses. Since Eddy current loss and hysteresis loss can be modeled as a function proportional to ω_e and a function proportional to the square of ω_e [13], respectively, the total operating loss is

Sheng-Ming Yang and Feng-Chieh Lin, Department of Mechanical Engineering, Tamkang University Tamshui, Taipei County, Taiwan 25137, Email: smyang@mail.tku.edu.tw

0-7803-7233-6/01/$10.00 ©2001 IEEE.

$$P=\frac{3}{2}\left[\left(i_{qs}^{e\,2}+i_{ds}^{e\,2}\right)r_s+\left(i_{qr}^{e\,2}+i_{dr}^{e\,2}\right)r_r+K_h\omega_e\lambda_m^{e\,2}+K_e\omega_e{}^2\lambda_m^{e\,2}\right] \quad (5)$$

where λ_m^e is the air-gap flux, K_e and K_h are the Eddy current and hysteresis loss coefficients. When the motor is running under the rotor flux field orientation and at steady state, $i_{dr}^e=0$ and $i_{qr}^e=-\frac{L_m}{L_r}i_{qs}$. Hence λ_m^e can be eliminated from Eq. (5), and the loss becomes

$$P=\frac{3}{2}\left[\left(i_{qs}^{e\,2}+i_{ds}^{e\,2}\right)r_s+\frac{L_m^{\,2}}{L_r^{\,2}}i_{qs}^{e\,2}+\left(K_h\omega_e+K_e\omega_e{}^2\right)\left(\frac{L_{lr}{}^2L_m{}^2}{L_r^{\,2}}i_{qs}^{e\,2}+L_m{}^2i_{ds}^{e\,2}\right)\right] \quad (6)$$

where L_r and L_m are the rotor and the mutual inductance, respectively. Since the rotor flux and the motor torque can be written as

$$\lambda_{dr}^e=L_m\,i_{ds}^e \quad (7)$$

$$T_e=\frac{3}{2}\frac{P}{2}\frac{L_m}{L_r}\lambda_{dr}^e i_{qs}^e \quad (8)$$

where T_e is the motor torque. Substituting Eqs. (7-8) into (6) to eliminate currents, then taking the derivative with respect to λ_{dr}^e on the resulting equation to find the minimum-loss rotor flux in terms of motor torque, yields

$$\lambda_{dr}^{e*}=\sqrt[4]{\frac{K_1}{K_2}}\,T_e^{\,0.5} \quad (9)$$

where $K_1=\frac{16}{3p^2}\left(r_r+K_e{r_r}^2+\frac{L_r^{\,2}}{L_m^{\,2}}r_s\right)$ and $K_2=3\left(\frac{r_s}{L_m^{\,2}}+K_h\omega_r+K_e\omega_r{}^2\right)$.

The above equation gives an expression for the exact minimum-loss rotor flux as a function of T_e. However, this control law is not practical because T_e is difficult to obtain in real time control. In the next section, a minimum-loss control scheme that uses the power factor as the primary control variable is described.

III. PRINCIPLE OF THE MINIMUM-LOSS CONTROL

Substituting Eqs. (7-8) into (1-2) to eliminate current and stator flux, then motor voltage and current in terms of torque and rotor flux can be written as

$$V_{qs}^e=a_0\lambda_{dr}^e\omega_r+a_1\frac{T_e}{\lambda_{dr}^e} \quad (10)$$

$$V_{ds}^e=-a_2\lambda_{dr}^e+a_3\frac{Te^2}{\lambda_{dr}^{e\,3}}+a_4\frac{T_e}{\lambda_{dr}^e}\omega_r \quad (11)$$

$$i_{qs}^e=a_5\frac{T_e}{\lambda_{dr}^e} \quad (12)$$

$$i_{ds}^e=a_6\lambda_{dr}^e \quad (13)$$

where a_0~a_6 are combinations of motor parameters and are given in Appendix A. Since the power factor is defined as

$$PF=Cos\theta=\frac{V_{qs}^e i_{qs}^e+V_{ds}^e i_{ds}^e}{\sqrt{V_{qs}^{e\,2}+V_{ds}^{e\,2}}\sqrt{i_{qs}^{e\,2}+i_{ds}^{e\,2}}} \quad (14)$$

Substituting Eqs. (10)-(13) into (14), then power factor can be written as a function of motor speed, rotor flux and torque as follows,

$$PF=\frac{\frac{4\omega_r}{3p}T_e+\frac{16}{9p^2}\left[r_s\frac{L_r^{\,2}}{L_m^{\,2}}+r_r\right](\frac{T_e}{\lambda_{dr}})^2+\frac{r_s}{L_m^{\,2}}\lambda_{dr}{}^2}{\sqrt{\left[a_0\lambda_{dr}^e\omega_r+a_1\frac{T_e}{\lambda_{dr}^e}\right]^2+\left[-a_2\lambda_{dr}^e+a_3\frac{Te^2}{\lambda_{dr}^{e\,3}}+a_4\frac{T_e}{\lambda_{dr}^e}\omega_r\right]^2}\times\sqrt{(a_5\frac{T_e}{\lambda_{dr}})^2+(a_6\lambda_{dr})^2}} \quad (15)$$

Finally, replace λ_{dr}^e with λ_{dr}^{e*} found in Eq. (9) yields

$$PF^*=\frac{\frac{4\omega_r}{3p}+\frac{16}{9p^2}\left[r_s\frac{L_r^{\,2}}{L_m^{\,2}}+r_r\right]\sqrt[4]{\frac{K_2}{K_1}}+\frac{r_s}{L_m^{\,2}}\sqrt[4]{\frac{K_1}{K_2}}}{\sqrt{\left[\sqrt[4]{\frac{K_1}{K_2}}a_0\omega_r+a_1\sqrt[4]{\frac{K_2}{K_1}}\right]^2+\left[-a_2\sqrt[4]{\frac{K_1}{K_2}}+a_3\sqrt[4]{\left(\frac{K_2}{K_1}\right)^3}+a_4\sqrt[4]{\frac{K_2}{K_1}}\omega_r\right]^2}\sqrt{a_5^2\sqrt[4]{\frac{K2}{K_1}}+a_6^2\sqrt[4]{\frac{K_1}{K_2}}}} \quad (16)$$

where PF^* is the minimum-loss power factor for a given T_e. Note that Eq. (16) is a function of motor parameters and ω_r only; the expression for PF^* does not contain T_e.

The above results can be illustrated with Fig. 1, where the motor operating loss and PF vs. i_{ds}^e under various output torque for a typical one horsepower motor running at 900 rpm are shown. The motor parameters can be found in Appendix B. As can be seen from Fig.1a) that the minimum-loss points, which are indicated with by 'o', varied for different T_e. But the power factor at the minimum-loss power points shown in Fig. 1b) are identical regardless of T_e. This is consistent with the result indicated by Eq. (16). Moreover, the minimum-loss power factors are generally located near the region where the slope of power factor vs. i_{ds}^e is steep, and they are away from the peak of the power factor vs. i_{ds}^e curves except at very low speeds.

Although the iron saturation was not considered in the derivation of Eq. (16), its effect is limited. This can be illustrated with the minimum-loss power factor vs. speed under various loads for the 1 hp motor shown in Fig. 2. Iron saturation was included in the calculations. It can be seen that only small variations occurred on the power factor as load varied, and the variations are too small for practical purpose. Therefore, iron saturation effect is neglected in this paper.

A minimum-loss power factor control for vector-controlled induction motor drives can be realized based on the previous results. Fig. 3 shows the block diagram of the controller. The relationship between PF^* and speed is calculated in advanced and stored as the references for the controller. The motor power factor is measured using Eq. (14); the error between the reference and the measured power factor is calculated and then regulated to zero by manipulating i_{ds}^e.

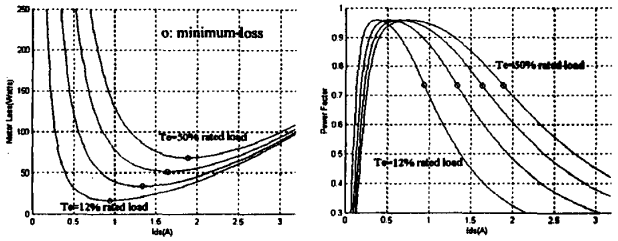

a) Total loss vs. i_{ds} b) Power factor vs. i_{ds}

Fig. 1. Operation loss and power factor vs. i_{ds} at various output torque for a typical 1 hp motor running at 900 rpm

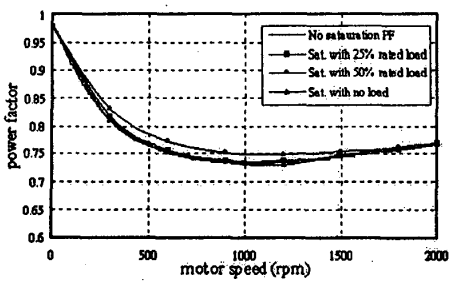

Fig. 2. Minimum-loss power factor vs. speed under various load for the 1 hp motor when the iron saturation is considered

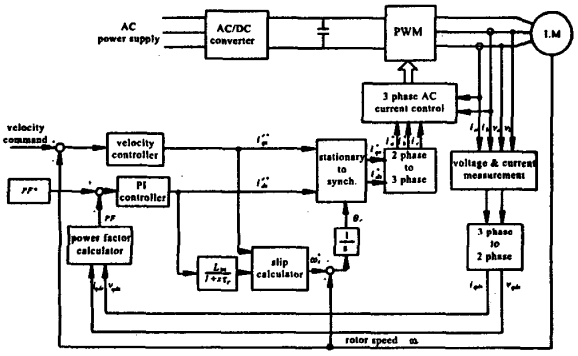

Fig. 3. Block diagram for the minimum-loss control system

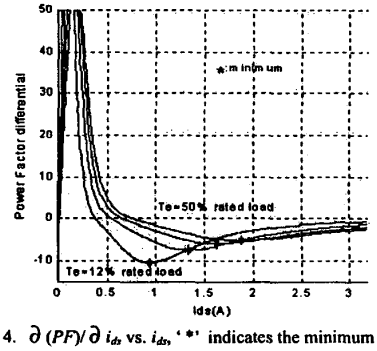

Fig. 4. $\partial (PF)/\partial i_{ds}$ vs. i_{ds}, '*' indicates the minimum value

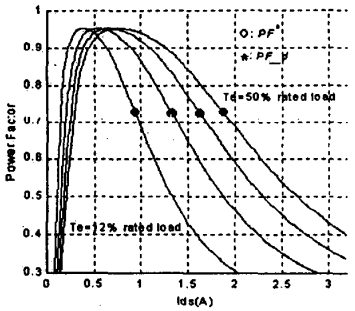

Fig. 5. Overlapping of PF_d on Fig. 1b)

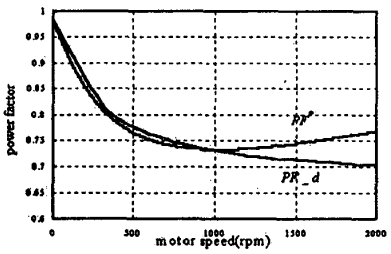

Fig. 6. Comparisons of PF^* and PF_d vs. motor speed for the 1 hp motor

Although the minimum-loss power factor can be calculated with Eq. (16), however, the calculation is quite difficult since the equation is complicated and requires motor parameters including K_h and K_e. Moreover, most of the previous reports were focused on the controller only, and how the power factor commands can be generated was not fully addressed[11,12]. In the following section, a scheme that allows automatic measurement of the optimal power factor commands is presented.

IV. MEASUREMENT OF MINIMUM-LOSS POWER FACTOR

Because the exact relationship between the minimum-loss power factor and speed is difficult to calculate, an approximate relationship that is easy for realization is proposed. As shown in Fig. 1b), most of the PF^* points occur near the region where the slope of PF vs. i_{ds}^e is minimized. To illustrate this observation, Fig. 4 shows the derivative of the power factor with respect to i_{ds}^e, i.e. $\partial (PF)/\partial i_{ds}$ vs. i_{ds}^e curves, where the minimum of these curves are denoted with '*'. Let the minimum of $\partial (PF)/\partial i_{ds}$ vs. i_{ds}^e be PF_d for convenience, it can be shown that PF_d also has the property similar to PF^* that it is a function of motor speed only when iron saturation is neglected. For comparison, the '*' points were superimposed on Fig. 1b) and then shown in Fig. 5. It can be seen that the '*' points are very close to the minimum-loss points. To be more specific, this result indicates that PF^* is approximately equal to PF_d for the 1 hp motor running at 900 rpm.

Fig. 6 shows both PF^* and PF_d vs. motor speed for the 1 hp motor. The two curves are very close to each other at

medium and low speeds, but have noticeable error at high speeds. Though this error is proportional to speed, however, it is still small comparing to the value of PF^*. Moreover, the error can be compensated easily since it is approximately a function of motor speed and PF_d. Therefore, in this paper, we proposed to use PF_d instead of PF^* for the optimal power factor command.

An advantage of using PF_d is that it can be found conveniently with automatic measurements. Fig. 7 illustrates the flow chart of the proposed PF^* measurement procedures. Because speed control is required, the measurement can be performed after the vector control and the velocity feedback loops are properly tuned. In the measurement, the motor is controlled to run from low to high speed with small steps. At each speed step, i_{ds}^e is also varied in small steps in order to calculate $\partial (PF)/\partial i_{ds}$. Since each $\partial (PF)/\partial i_{ds}$ vs. i_{ds}^e curve has a distinct minimum, i_{ds}^e only need to be varied till the minimum is found. After each PF_d is found, a compensation value, i.e PF_c, is calculated and then added to PF_d. The compensation scheme will be described in the next section. The sum of PF_d and PF_c is the calculated minimum-loss power factor. Note that since iron saturation is neglected, the measurement can be performed at no load. This has greatly simplified the measurement procedures and allowed them to be implemented as part of the auto-commissioning of the motor drive.

V. FUZZY LOGIC COMPENSATION

Several fuzzy logic based efficiency controller has been reported previously [3]. A fuzzy logic controller essentially embeds the experience and intuition of a human plant operator, and sometimes those of the designer of the plant. It is a knowledge-based system consisting of IF-THEN rules to mimic human thinking and a fuzzy inference mechanism for input and output variables. Hence, fuzzy logic is most suitable for the processes with complex nonlinear and parameter variation problems. Because the error between PF_d and PF^* is a nonlinear function of motor speed and also varying with motor size, a fuzzy logic compensator is employed to compensate for the error.

Fig. 8 illustrates the basic structure of the proposed fuzzy compensator. The compensator uses PF_d and ω_r as its inputs, and outputs a correction term, i.e. PF_c, for the power factor command. Let the calculated minimum-loss power factor be PF_o, then

$$PF\_o = PF\_d + PF\_c \tag{17}$$

Each input/output of the fuzzy compensator has an associated set of membership functions that maps the input/output space to a degree of membership. Fig. 9 shows these membership functions. Each membership function set contains five individual membership functions, and that is: negative big (NB), negative small (NS), approximately zero (ZE), positive small (PS), and positive big (PB). All membership functions are triangular for simplicity. The compensator output is calculated with the centroid de-fuzzification method.

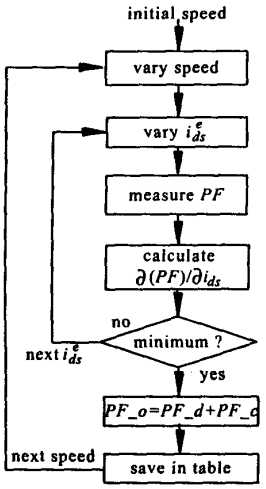

Fig. 7. Procedures for automatic measurement of the minimum-loss power factor commands

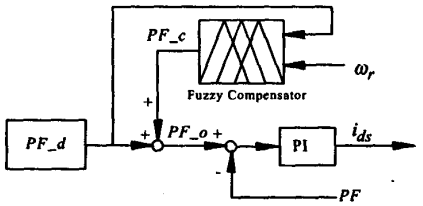

Fig. 8. Block diagram for the fuzzy logic power factor compensator

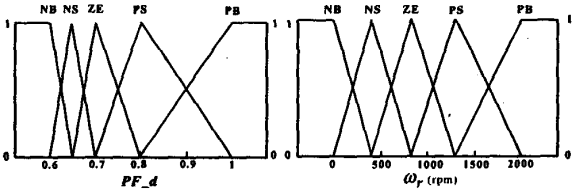

a) Power factor command input b) Velocity input

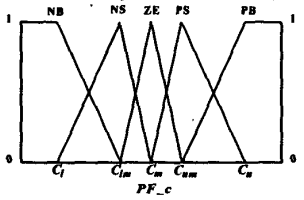

(c) Compensator output

Fig. 9. Membership functions of the fuzzy power factor compensator

The input range for PF_d is set to between 0.6 and 1.0 for motors above 1 hp. Because PF_d is most likely to fall into the lower input space, i.e. typically between 0.7~0.8, its membership functions are designed to center at a lower PF_d to increase its sensitivity. Similarly, the input range for ω_r is set to between 0 and the rated speed of the motor, and its membership functions are also centered at a lower input since

the relationship between PF^* and ω_r has more disproportion at low speeds.

On the other hand, the output membership function is symmetric about zero since both the position and the negative PF_c is required. However, because the error between PF_d and PF^* varied with motor size, the upper and the lower bounds of the output membership functions must also varied accordingly in order to get proper correction value. Fig. 10 illustrates the upper and the lower bounds for the motors ranging from 1 to 50 hp. Both bounds are linearly proportional to motor size. Then, the ranges for the output membership functions can be found with the following function,

$$\begin{bmatrix} C_u \\ C_{mu} \\ C_m \\ C_{ml} \\ C_l \end{bmatrix} = \begin{bmatrix} 1 \\ 0.667 \\ 0.5 \\ 0.333 \\ 0 \end{bmatrix} * (C_u - C_l) + C_l \qquad (18)$$

where C_u, C_{mu}, C_m, C_{ml}, and C_l are shown in Fig. 9.

The fuzzy compensator has 25 rules, as shown in Table 1. These rules are constructed according to the experience of how the power factor should be corrected according to the nonlinear relationship between PF^*, PF_d and speed.

Fig. 11 shows the simulated PF_o, PF_c, and PF_d for 1, 10, 20, and 50 hp motors, respectively. These motors are typical induction servomotors, and their parameters can be found in Appendix B. It can be seen that all the calculated power factors are very close to the theoretical minimum-loss power factors. The largest error was around 0.03 for the 50 hp motor. But the error is negligible for practical purpose since the loss vs. i_{ds}^e curve is flat near the minimum-loss point.

VI. Experiment Results

The minimum-loss control scheme presented in the previous sections was implemented with a TMS320C240 DSP based development system to control the 1 hp induction motor shown in Appendix B. Vector control of the motor was implemented to assist the verification of the minimum-loss control scheme. Both d and q axis voltages and currents were measured and filtered so that only the fundamental components were read by the DSP for the power factor calculation. The fuzzy compensation values were pre-calculated and implemented as a table in the controller to reduce the execution time.

Fig. 12 shows the experimental results when the motor was running at 900 rpm and 25% rated load. In the beginning of the experiment, i_{ds}^e was fixed to its rated value. Then the minimum-loss control was switched on at approximately 2.5 seconds. The minimum-loss power factor for this motor running at 900 rpm is around 0.73. As can be seen from Fig. 12 that the power factor was 0.45 initially, and then converged to 0.73 after the control was on. Notice the transient responses were quite smooth before the motor reached its steady state. Although only the responses for 900 rpm were shown, similar results can be obtained for other speeds.

Fig. 14 shows the energy savings the minimum-loss control can achieve. The input power when the motor was running at various speeds and under 25% and 50 % rated load, respectively, were measured. As can be seen that only about 3% savings was obtained when the load was 50% of its rated value. However, nearly 17% savings was obtained when the load was 25% of the rated value. Though this result is well known, but it has confirmed that the proposed control scheme is effective in minimizing the motor operating loss.

VII. Conclusions

A minimum-loss control scheme for vector-controlled induction motor drives was proposed in this paper. The control scheme utilizes the motor power factor as the main control variable and manipulates the magnetizing current in order for the motor to operate at its minimum-loss point. In conjunction with the power factor control, a scheme for the measurement of the optimal power factor command was proposed. The main advantage of this scheme is that it is simple for implementation and does not require an a priori knowledge of the motor parameters. The experimental results have confirmed the effectiveness of the control scheme in controlling the motor to its minimum-loss condition regardless of load variations.

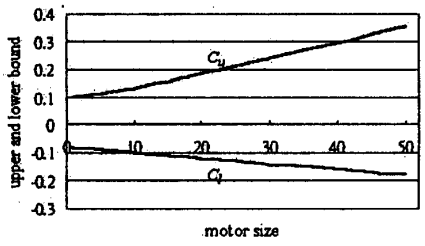

Fig. 10. Upper and lower bounds of the output membership function

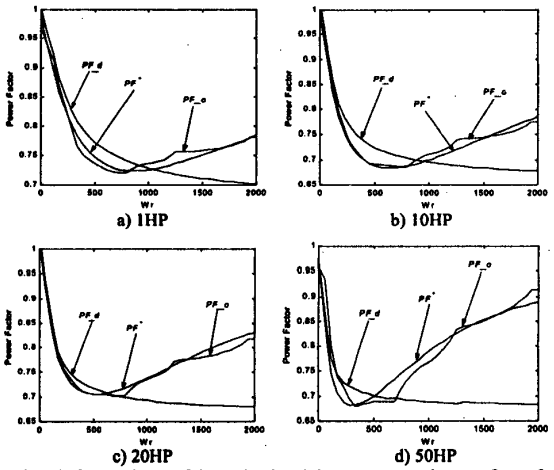

Fig. 11. Comparisons of the optimal and the compensated power factor for various motors

ω_r / PF_d	NB	NS	ZE	PS	PB
NB	PS	ZE	ZE	PS	PB
NS	ZE	NS	NS	ZE	PS
ZE	ZE	NB	NS	ZE	ZE
PS	ZE	NB	NB	NS	NS
PB	NS	NB	NB	NB	NB

Table 1 Rule base for the fuzzy power factor compensator

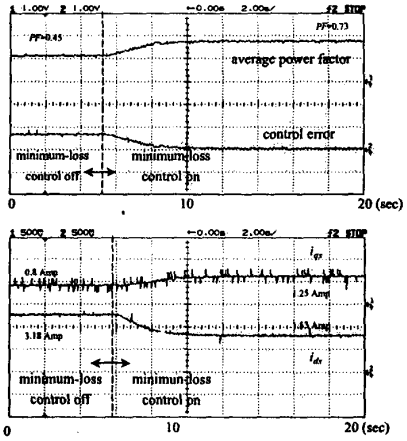

Fig. 12. Power factor and current responses before/and after the minimum-loss control was applied, the motor was running at 900 rpm and 25% rated load

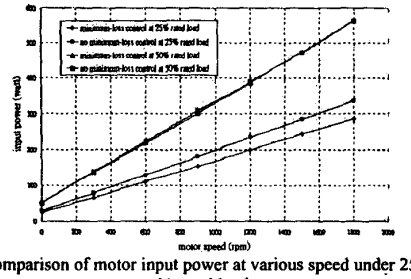

Fig. 13. Comparison of motor input power at various speed under 25% and 50 % rated load

APPENPIX A

$$a_0 = (\frac{L_m}{L_r} + \sigma \frac{L_s}{L_m}) \quad , \quad a_1 = \frac{4}{3P}(r_r(\frac{L_m}{L_r} + \sigma \frac{L_s}{L_m}) + \frac{L_r}{L_m} r_s) \quad ,$$

$$a_2 = \frac{r_s}{L_m} \quad , \quad a_3 = \frac{16\sigma}{9P^2} \frac{L_s L_r r_r}{L_m} \quad , \quad a_4 = \frac{4\sigma}{3P} \frac{L_s L_r}{L_m} \quad , \quad a_5 = \frac{4}{3p} \frac{L_r}{L_m} \quad ,$$

$$a_6 = \frac{1}{L_m}$$

APPENPIX B

All the motors are 3 Phase, 4 Poles, 66Hz, 2000 rpm, the parameters are:

	r_s (ohm)	r_r (ohm)	L_s (H)	L_r (H)	L_m (H)	K_h	K_e	Voltage
1 hp	5.23	2.4	0.1908	0.1940	0.1876	87e-5	87e-5	220
10 hp	0.566	0.384	0.0416	0.0420	0.0406	41e-5	41e-5	220
20 hp	0.332	0.153	0.0322	0.0325	0.0315	58e-5	58e-5	380
50 hp	0.064	0.038	0.0134	0.0135	0.0133	153e-4	153e-4	380

ACKNOWLEDGEMENTS

We gratefully acknowledge the support for this research by the National Science Council, Taiwan, R. O. C., under grant: NSC 89-2213-E-032-041.

REFERENCES

[1] Kirschen D.S., Novotny D.W. and Lipo T.A., "Optimal Efficiency Control of an Induction Current Source Inverter Fed Induction Motor," *Proceedings of the IEEE-PESC*, pp.486-493, 1986.

[2] Cleland J., MacCormick V. and Wayne Turner M., "Design of an Efficiency Optimization Controller for Inverter-Fed ac Induction Motors," *Conference Record of the IEEE IAS Annual Meeting*, pp.16-21, 1995.

[3] Gilberto C.D.S., Bimal K.B. and John G.C., "Fuzzy Logic Based On-Line Efficiency Optimization Control of an Indirect Vector-Controller Induction Motor Drive," *IEEE Trans. on IE*, Vol.42, pp.192-198, 1995.

[4] Blaabjerg F. and Pedersen J.K., "An Integrated High Power Factor Three-Phase AC-DC-AC Converter for Ac-Machines Implemented in One Microprocessor," *Proceedings of the IEEE-PESC*, pp.285-292, 1993.

[5] Famouri P. and Cathey J.J., "Loss Minimization Control of an Induction Motor Drive," *IEEE Trans. on IAS*, Vol.27, pp.32-37, 1991.

[6] Iordanis Kioskeridis and Nikos Margaris, "Loss Minimization in Induction Motor Adjustable-Speed Drives," *IEEE Trans. on IE*, Vol.43, pp.226-231, 1996.

[7] Kusko A. and Galler D., "Control Means for Minimization of Losses in ac and dc Motor Drives," *IEEE Trans. on IAS*, Vol.19, pp.561-570, 1983.

[8] Garcia G.O., Mendes Luis J.C., Stephan R.M. and Watanabe E.H., "An Efficient Controller for an Adjustable Speed Induction Motor Drive," *IEEE Trans. on IE*, Vol.41, pp.533-539, 1994.

[9] Sul S.K. and Park M.H., "A Novel Technique for Optimal Efficiency Control of Motor Drive," *IEEE Trans. on Energy Conversion*, Vol.EC-2, pp.70-76, 1987.

[10] Kim H.G., Sul S.K. and Park M.H., "Optimal Efficiency Drive of a Current Source Inverter Fed Induction Motor by Flux Control," *IEEE Trans. on IAS*, Vol.IA-20, pp.1453-1459, 1984.

[11] Nola F., "Power Factor Controller - An Energy Saver," *Conference Record of the IEEE IAS Annual Meeting*, pp.194-198, 1980.

[12] Anderson, H.R. and Pedersen, J.K., "Low Cost Energy Optimized Control Strategy for a Variable Speed Three-Phase Induction Motor," *Proceedings of the IEEE-PESC*, pp.920-924, 1996.

[13] Kirschen D., Novotny D.W. and Suwanwisoot W., "Minimizing Induction Motor Losses by Excitation Control in Variable Frequancy Drives," *IEEE Trans. on IAS*, Vol.20, pp.1244-1250, 1984.